# Observation of Quenching in Gamow-Teller Strength in the (p,n) Reaction on sd-Shell Nuclei

|  |  |
|---|---|
| 著者 | Orihara H., Furukawa K., Kabasawa M., Kawamura T., Takahashi Y., Niizeki T., Maeda K., Nakagawa T., Miura K., Ohnuma H. |
| journal or publication title | CYRIC annual report |
| volume | 1984 |
| page range | 22-28 |
| year | 1984 |
| URL | http://hdl.handle.net/10097/49209 |

# I. 5 Observation of Quenching in Gamow-Teller Strength in the (p,n) Reaction on sd-Shell Nuclei

Orihara H., Furukawa K.*, Kabasawa M.*, Kawamura T.*, Takahashi Y.*, Niizeki T., Maeda K.**, Nakagawa T.*, Miura K.*** and Ohnuma H.****
Cyclotron and Radioisotope Center, Tohoku University
Department of Physics, Faculty of Science, Tohoku University*
College of General Education, Tohoku University**
Tohoku Institute of Technology***
Department of Physics, Tokyo Institute of Technology****

While many authors have suggested[1], for the quenching of the spin-isospin excitation, that Δ-isobar admixture entering into the nuclear wave function plays an important role, others have suggested[2,3] that the data may be understood in terms of only nucleon degrees of freedom once a configuration mixing, which includes adequate model spaces, is taken into account. From the view points of experimental data on GTGR, on the other hand, reduction of cross sections for which is always suffered from ambiguity for the back-ground subtraction. Indeed, the recent estimation by Osterfeld et al., has shown that a significant fraction of spin-flip component is buried in the continuum part of the intermediate energy (p,n) spectrum.[4]

Recently, Anantaraman and his collaborators have reported[5] a striking results on quenching in isovector $0^+ \rightarrow 1^+$ transitions in $^{28}$Si(p,p'). Their points are twofold; 1) reduction factors of the cross sections are almost identical of 30% for both isoscalar and isovector channel, 2) the factor for the ΔS=1, ΔT=1 channel is inconsistent with that obtained by the (e,e') experiment. Thus, a systematic study for, at least, the isovector $0^+ \rightarrow 1^+$ transition, expected to be excited in a much simpler manner than the isoscalar one, is strongly awaited for, in order to make comprehensive comparison among data from different probes, then to make clear the origin of the quenching.

The (p,n) Gamow-Teller transitions in sd-shell nuclei are potentially richer candidate proving the quenching of the spin-isospin channel due to; 1) there exist a number of quite strong $\Delta J^\pi=1$, $0^+ \rightarrow 1^+$ transitions concentrated to low-lying levels, 2) shell model wave functions are available established by Wildenthal and Brown through stringent tests.[6,7] In this report, we report a systematic study of the $0^+ \rightarrow 1^+$ transition by the charge exchange (p,n) reaction at $E_p$ = 35 MeV on sd-shell nuclei covering almost all even-even targets in this region. Among them, $^{24}$Mg, $^{28}$Si and $^{32}$S (N=Z) provide $0^+ \rightarrow 1^+$ transition capable for comparison with the results from (p,p') or (E,e') since only T=1 states are populated in the (p,n) reaction, while $^{18}$O, $^{22}$Ne, $^{26}$Mg, $^{30}$Si and $^{34}$S (N>Z) suffice the present purpose obtaining the correspondence between the quenching factors for the (p,n) reaction and for β-decay, since in case of the (p,n) reaction on a N=Z+2 nucleus the analog β-decay is easily found with its well known log ft value[8]; namely, ${}_{Z-1}A_{N+1} \rightarrow {}_{Z}A_{N}$ for (p,n) and ${}_{Z+1}A_{N-1} \rightarrow {}_{Z}A_{N}$ for β-decay.

The experiment was performed with use of a 35-MeV proton beam from the azimuthally varying field cyclotron and the time-of-flight facilities at the Cyclotron and Radioisotope Center, Tohoku University. We have utilized a beam swinger system, and measured angular distributions of emitted neutrons between 0° and 140° (lab.). Enriched ${}^{18}$O(99%) or ${}^{22}$Ne(99%) gas was filled in a gascell with natural calcium windows. The ${}^{24,26}$Mg targets were prepared by rolling metallic magnesium enriched to $\gtrsim$99.9% in ${}^{24}$Mg and ${}^{26}$Mg. A silicon wafer with natural isotopic abundance was used as the ${}^{28}$Si target, while $SiO_2$ and elemental sulphur powder enriched to 98, 99.9 and 99.9% in ${}^{30}$S, ${}^{32}$S and ${}^{34}$S, respectively, were evaporated onto enriched ${}^{12}$C foils. The thicknesses of these targets were respectively, 1.50, 1.83, 3.40, 2.33, 2.12, 0.46, 1.48 and 2.2 mg/cm$^2$ for ${}^{18}$O, ${}^{22}$Ne, ${}^{24}$Mg, ${}^{26}$Mg, ${}^{28}$Si, ${}^{30}$Si, ${}^{32}$S and ${}^{34}$S. Overall time resolution was 1.3 nsec. The errors in the absolute cross section are estimated to be $\sim$15%, while relative errors are $\sim$7%. Further details of the experiment are given in our previous papers.[9]

Figures 1(a) and (b) show representative neutron energy spectra obtained from time-of-flight measurements for N=Z (on ${}^{28}$Si) and N=Z+2 (on ${}^{34}$S) targets, respectively. Especially, the ${}^{28}$Si(p,n)${}^{28}$P reaction is expected to resolve the discrepancy in the quenching factor for the electromagnetic transitions and for the hadron scattering[5] as described earlier. In the bottom of each figure, the GT-strength distributions evaluated by the one body transition density matrix elements by Wildenthal, Brown and Chung (WBC-OBTD)[6,7] are intercepted for comparison. The excitation energies of the predicted $1^+$ states are drawn so as to match the observed locations, which coincide with those reported by Anderson et al.[10] in their work on the ${}^{28}$Si(p,n)${}^{28}$P reaction at $E_p$ = 135 MeV. Figures 1(a) and (b) readily show that the GT strength in a sd-shell nucleus strongly concentrate on one or two, usually on one level, and also show that the WBC-OBTD matrix elements give, indeed, fairly good accounts for the general feature of the $0^+ \rightarrow 1^+$ (p,n) transition strength distribution.

Figures 2(a) and (b) illustrate the angular distributions of emitted neutrons leading to the four $1^+$ states in the residual nuclei of ${}^{28}$P and ${}^{34}$Cl, respectively, together with the DWBA predictions obtained by the M3Y interactions by Bertsch et al.[11], and the WBC-OBTD matrix elements. These angular distribution shapes show specific aspects that many of them have a peak around $\theta_{C.M.} \simeq 25°$, and that others exceptionally have a steep forward peaked pattern. The former angular distribution is similar to that of the $0^+ \rightarrow 0^+$ (pure ΔL=0) analog transition easily observed in the N>Z case, while the latter one, an example for which is the $0^+ \rightarrow 1^+$ transition to the 0.66 MeV state in ${}^{34}$Cl, is quite similar to that of the $0^+ \rightarrow 2^+$ (pure ΔL=2) analog transition, for example, to the $E_x$ = 3.38 MeV, $2^+$ and T=1 state in ${}^{34}$Cl. In order to make sure that $\Delta L=0$ is the major part for the former case and $\Delta L=2$ for the latter, we have calculated $\sigma(\Delta L=0)$ and $\sigma(\Delta L=2)$ separately as illustrated in Fig. 2(b). Comparison is satisfactory, and it leads us to a conclusion that some of the low-energy (p,n) transition exhibit too large cross sections, especially at small angles, than those expected from the corresponding B(GT) value, however careful measurements of their angular distributions enable us to reject the mixture of the L=2 component. Furthermore, the $\Delta L=1$ component, encountered through the exchange part, contribute negligibly as shown by a dotted line in Fig. 2(b). It should be remarked that the WBC-OBTD matrix elements predict the (p,n) cross sections consistently not only for the $\Delta L=0$ favoured GT transitions but also for the $\Delta L=2$ dominated ones.

DWBA calculations in Fig. 2(a) and (b) are multiplied by normalization factors to produce the fits to the data. The reduction factors, thus obtained for (p,n) [$\sigma_{exp.}/\sigma_{cal.}$ (at peak around $\theta^{C.M.}=25°$)], listed in the last column of Table 1, which also tabulate information about $\beta$-decays which are analogous to the present (p,n) transition of N=Z+2 targets. As for the reduction factors for $\beta$-decay obtained from the free-nucleon value, Brown and Wildenthal$^{7)}$ have given their implication by empirical normalization factors of the $\underline{\ell}$, $\underline{s}$, and $[\underline{Y}^{(2)}\otimes\underline{s}]^{(1)}$ single-particle operators by taking into accounts the recent calculations, by Towner and Kahanna, where correlations to the above mentioned free-nucleon value are considered about the effects of isobar current, meson-exchange current and mixing with configurations outside the sd-shell. We should not discuss details on $\beta$-decay further, except that we will emphasize that the (p,n) reduction factors are quite close to those from $\beta$-decay; the average quenching for $\beta$-decay is 0.58(-24%), while this is 0.51(-29%) for the GT (p,n) reaction, thus suggesting the issue of the sources of the phenomena may be common. Hence, $V_{\sigma\tau}$ should be changed, as much as $g_A$ corrected by speculation mentioned above.

One-to-one comparison has been discussed by the data listed in Table 1. However, in some cases, especially for the N=Z cases, comparison is improved when we take the sum of the (p,n) cross sections leading to more than two $1^+$ states as listed in Table 2. The most striking feature of this table is the reduction factor on the $^{28}$Si(p,n)$^{28}$P reaction indicating it is 0.72(-15%), indeed being consistent with the electromagnetic transitions which have yielded the results of 0.7-0.77.$^{12)}$ We may read in Table 2 another example on $^{24}$Mg, where the reduction factor is 0.73 capable for comparison with the data on electromagnetic transitions giving the factors lying in 0.7.$^{6)}$

In conclusion a systematic study, for the $0^+ \rightarrow 1^+$ transition, has been carried out through the (p,n) reaction on sd-shell nuclei. A number of the GT-transitions have been observed, and their differential cross sections were compare with the DWBA predictions calculated by using spectroscopic amplitudes obtained by the full sd-shell based WBC-OBTD matrix elements. Deduced quenching factors have been discussed in two cases; they were compared with results from (e,e') and (p,p') experiments in the samples of the N=Z targets, while they were compared with the β-decay matrix elements in the N>Z targets. In the almost all (p,n) reaction observed, their quenching factors were consistent with the previous results from other experiments. Especially, for the N>Z case, the quenching factors in the (p,n) reaction deduced by the DWBA analysis with the M3Y interactions, where the free N-N interaction were taken into accounts, were as large as those in β-decay by the free $(g_A/g_V)$ ratio.

## References

1) See for example, Brown G. E. and Rho M., Nucl. Phys. A372 (1981) 397.
2) Arima A., in Spin Excitations in Nuclei, edited by Petrovichi F. et al., (Plenum, New York, 1984), p. 7 and references there in.
3) Amusa A. and Lawson R. D., Phys. Rev. Lett. 51 (1983) 103.
4) Osterfeld F., Cha D. and Speth J., Phys. Rev. C 31 (1985) 372.
5) Anantaraman N. et al., Phys. Rev. Lett. 52 (1984) 1409.
6) Brown B. A. and Wildenthal B. H., Phys. Rev. C 27 (1983) 1296.
7) Brown B. A. and Wildenthal B. H., Phys. Rev. C 28 (1983) 2397.
8) Endt P. M. and Van der Leun C., Nucl. Phys. A310 (1978) 1.
9) Orihara H. and Murakami T., Nucl. Instrum. and Methods 188 (1981) 15.
10) Anderson B. D. et al., Phys. Rev. 27 (1983) 1387.
11) Bertsch G. et al., Nucl. Phys. A284 (1977) 399.
12) Schneider et al., Nucl. Phys. A323 (1979) 13.

Table 1. Quenching factors both in the β-decay and (p,n) reaction.

| $\beta^+$-decay | | | Shell-Model (WBC-OBTD) | Quenching Factor | |
|---|---|---|---|---|---|
| Initial State(g.s.) | Final State ($E_x$ in MeV) | B(GT) | B(GT)[a] | $\varepsilon_\beta$[b] | $\varepsilon_{(p,n)}$[c] |
| $^{18}$F | $^{18}$O (0.0) | 1.62 | 2.63 | 0.62 | 0.47 |
| $^{22}$Mg | $^{22}$Na(0.583) | 1.38 | 2.53 | 0.55 | 0.53 |
| $^{22}$Mg | $^{22}$Na(1.937) | 2.29 | 3.66 | 0.63 | 0.55 |
| $^{26}$Si | $^{26}$Al(1.06) | 1.82 | 2.99 | 0.61 | 0.61 |
| $^{26}$Si | $^{20}$Al(1.85) | 0.92 | 1.36 | 0.70 | 0.42 |
| $^{30}$S | $^{30}$P (3.02) | 1.95 | 3.56 | 0.55 | 0.51 |
| $^{34}$Ar | $^{34}$Cl(3.13) | 2.19 | 4.04 | 0.54 | 0.45 |

a) Except for the case of $^{18}$F-$^{18}$O, these β decays have the same initial and final states with the (p,n) reaction, but they are analog transitions to the corresponding $\beta^+$ decay.

b) $\varepsilon_\beta = \dfrac{\text{B(GT)[experimental } \beta^+ \text{ decay]}}{\text{B(GT)[Shell-Model value with free nucleon } \langle\sigma\tau\rangle]}$ .

c) $\varepsilon_{(p,n)} = \dfrac{d\sigma/d\Omega\text{[experimental cross section]}}{d\sigma/d\Omega\text{[DWBA value with M3Y]}}$ .

Table 2. Comparison of observed $0^+ \rightarrow 1^+$ transitions in the (p,n) reaction on the sd-shell nuclei with the shell-model by Wildenthal, Chung and Brown.

| Target | #[a] | Theory<br>B(GT)[b] | <br>dσ/dΩ[c]<br>(mb/sr) | (p,n)<br>$E_x$<br>(MeV) | <br>dσ/dΩ[d]<br>(mb/sr) | Quenching |
|---|---|---|---|---|---|---|
| $^{18}$O | 1 | 7.91 | 7.4 | 0.0 | 3.41 | |
| | 3 | 0.080 | 0.3 | 3.72 | 0.66 | |
| | | | Σ = 7.70 | | Σ = 4.07 | 0.53 |
| $^{22}$Ne | 1 | 2.53 | 1.91 | 0.58 | 1.01 | |
| | 2 | 3.66 | 3.17 | 1.94 | 1.75 | |
| | | | Σ = 5.08 | | Σ = 2.85 | 0.56 |
| $^{24}$Mg | 2 | 1.51 | 0.74 | 1.12 | 0.58 | |
| | 3 | 0.82 | 0.42 | 3.02 | 0.26 | |
| | | | Σ = 1.16 | | Σ = 0.84 | 0.72 |
| $^{26}$Mg | 1 | 2.99 | 1.96 | 1.06 | 1.20 | |
| | 2 | 1.36 | 1.41 | 1.85 | 0.60 | |
| | | | Σ = 3.58 | | Σ = 2.14 | 0.53 |
| $^{28}$Si | 1 | 0.0061 | 0.04 | 1.13 | 0.13 | |
| | 2 | 0.98 | 0.42 | 1.52 | 0.16 | |
| | 3 | 1.21 | 1.11 | 2.13 | 0.82 | |
| | | | Σ = 1.57 | | Σ = 1.11 | 0.71 |
| $^{30}$Si | 3 | 3.56 | 1.97 | 3.04 | 1.01 | 0.51 |
| $^{32}$S | 2 | 0.69 | 0.32 | 1.11 | 0.20 | |
| | 6 | 1.20 | 0.51 | 3.83 | 0.32 | |
| | 7 | 1.72 | 0.81 | 4.03 | 0.30 | |
| | | | Σ = 1.64 | | Σ = 0.82 | 0.50 |

a) Same with # in; B. H. Wildenthal and W. Chung, in The (p,n) Reaction and the Nucleon-Nucleon Force, ed. by C. D. Goodman et al., (Plenum, New York, 1980) p. 89.

b) $B(GT) = \left| \sum_{jj'} \mathrm{OBTD} \cdot \langle j' || \sigma || j \rangle 1.251 \right|^2 \times \frac{1}{(2J_i+1)}$, where $\langle j' || \sigma || j \rangle$ is the free-nucleon value.

c) Obtained by DWBA calculations with M3Y interactions by using the OBTD's.

d) Peak differential cross section near $\theta_{C.M} = 30°$.

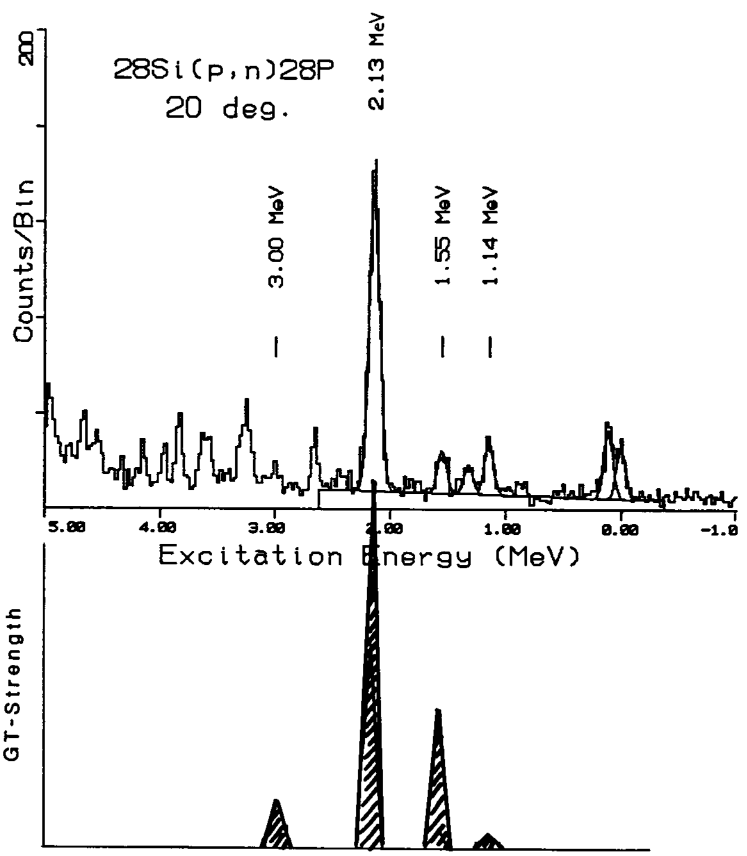

Fig. 1(a). A typical neutron spectrum of the case for the $^{28}$Si(p,n)$^{28}$P reaction at $\theta_L = 20°$. Peaks with excitation energies stand for the $0^+ \rightarrow 1^+$ transitions. Inserted in the bottom of the figure is GT-strength distribution calculated by the WBC-OBTD matrix elements.

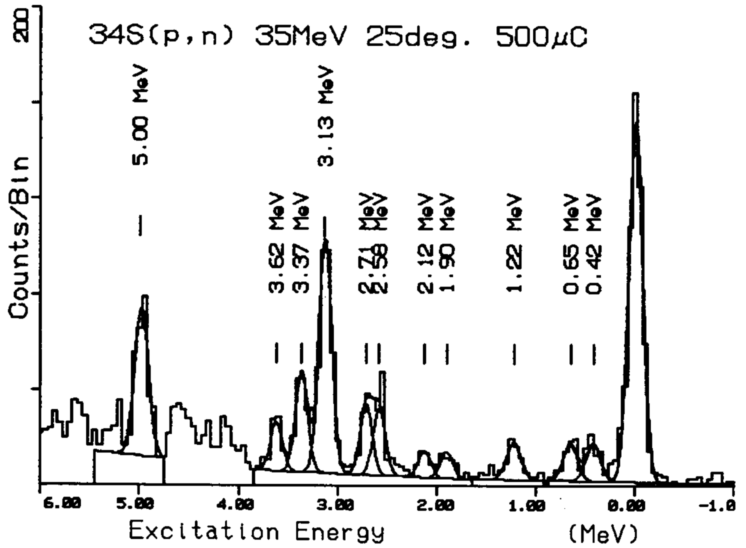

Fig. 1(b). Same with Fig. 1(a) but for the $^{34}$S(p,n)$^{34}$Cl reaction, and for $\theta_L = 25°$.

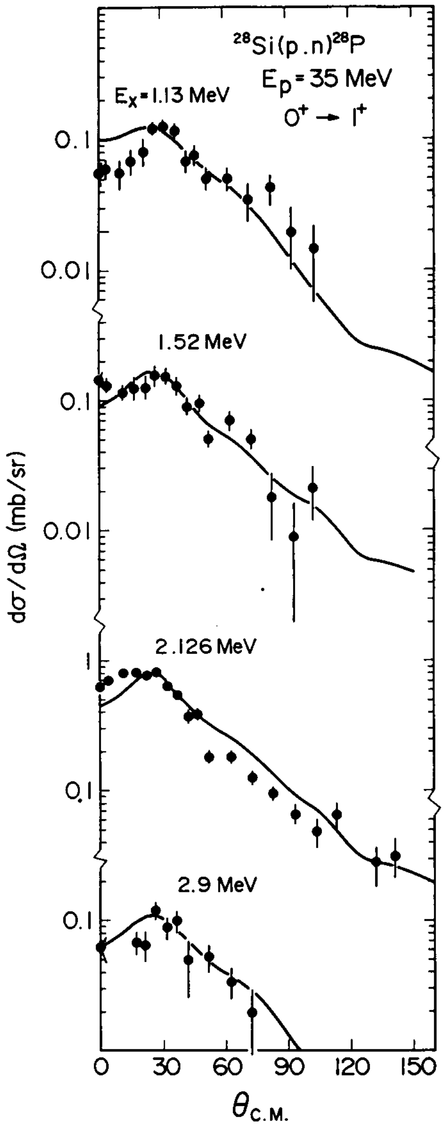

Fig. 2(a). Differential cross sections for the $0^+ \rightarrow 1^+$ transitions in the $^{28}$Si(p,n)$^{28}$P reaction. Lines show the DWBA comparison with use of the WBC-OBTD matrix elements and the M3Y interactions. Theoretical curves are normalized to the data in order to optimize the fitting by the quenching factor in Table 2.

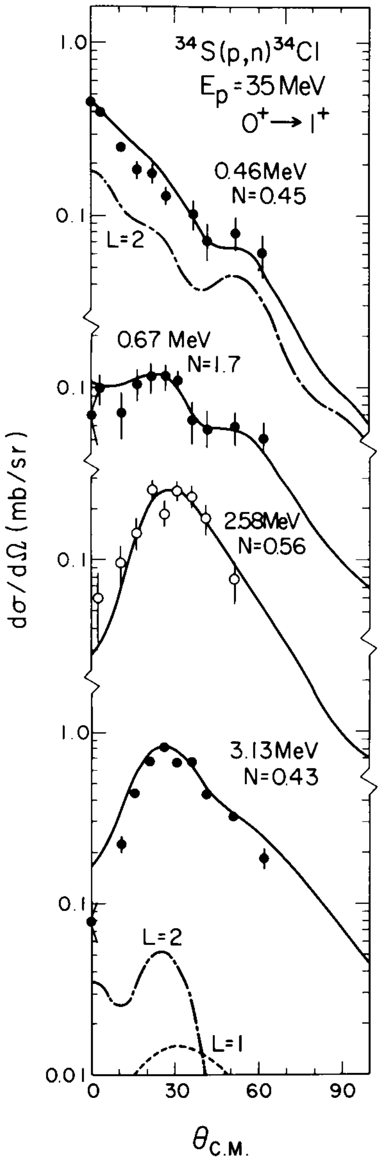

Fig. 2(b). Differential cross sections for the $0^+ \rightarrow 1^+$ transitions in the $^{34}$S(p,n)$^{34}$Cl reaction. Lines show DWBA predictions, where dash-dotted curves mean the L=2 contribution in a $\Delta J^{\pi} = 1^+$ transition, while the L=1 (dashed curve) component comes only through the exchange contributions.